2009-08MV-4

Health Monitoring for Condition-Based Maintenance of a HMMWV using an Instrumented Diagnostic Cleat

Tiffany DiPetta, David Koester, and Douglas E. Adams, Ph.D.
Center for Systems Integrity, Purdue University, 1500 Kepner Drive, Lafayette, IN 47905

Joseph Gothamy, Paul Decker, David Lamb, Ph.D., and David Gorsich, Ph.D.
Tank Automotive Research, Development and Engineering Center, Warren, MI 48397-5000

ABSTRACT

Operation & support costs for military weapon systems accounted for approximately 3/5th of the $500B Department of Defense budget in 2006. In an effort to ensure readiness and decrease these costs for ground vehicle fleets, health monitoring technologies are being developed for Condition-Based Maintenance of individual vehicles within a fleet. Dynamics-based health monitoring is used in this work because vibrations are a passive source of response data, which are global functions of the mechanical loading and properties of the vehicle. A common way of detecting faults in mechanical equipment, such as the suspension and chassis of a ground vehicle, is to compare measured operational vibrations to a reference (or healthy) signature to detect anomalies. The main difficulty with this approach is that many vehicles are not equipped with sensors or the acquisition systems to acquire, process, and store data; therefore, to implement health monitoring, one must overcome the economic and technical barriers associated with equipping ground vehicles to continuously monitor the response. The research in this paper explores one approach that aims to overcome this difficulty. If a vehicle cannot be equipped with sensors, then an instrumented diagnostic cleat is proposed to measure the dynamic response of the vehicle as it traverses the cleat at a fixed speed. This approach could be effective because it eliminates the need for on-vehicle sensors, but provides measurements that indicate the condition of wheels/suspensions. A simple model of a HMMWV is used to simulate the approach. Experiments are also conducted using an instrumented cleat to demonstrate the feasibility of this approach.

INTRODUCTION

The U.S. Army is pursuing technologies that will enable Condition-Based Maintenance (CBM) of ground vehicles. Current maintenance schedules for ground vehicles are determined based on reliability predictions (e.g., mean time to failure) of a population of vehicles under anticipated operational loads; however, vehicles that experience component damage often lie in the tails of the reliability distribution for a given platform. For example, a certain group of vehicles may be deployed to operate on a harsh terrain that is particularly taxing on the mechanical components in the suspensions or frames of those vehicles. Operation & support costs for military weapon systems accounted for approximately 3/5th of the $500B Department of Defense budget in 2006 (Gorsich, 2007). To ensure readiness and decrease these costs for ground vehicle fleets, health monitoring technologies are being developed to assess the reliability of individual vehicles within each fleet.

Based on a review of the open literature including Technical Note 85-3 (Thomas, 1985) on ground equipment reliability issues associated with materials, it can be concluded that the most common faults occur in wheel ends (tires, brakes), suspensions, and frames. For example, Aardema (1988) discussed a ball joint failure in the HMMWV (High Mobility Multi-purpose Wheeled Vehicle). Braking systems have also experienced wear most likely due to severe operating conditions such as overheating. Reliability issues in suspensions due to wheel weights have also been reported (FORSCOM, 2004). Faults in the HMMWV body chassis and frame have also been reported in reliability centered maintenance studies (Lasure, 2004).

Dynamics-based health monitoring is used in this work to identify such faults because vibrations are a passive source of response data, which are global functions of the loading and mechanical properties of the vehicle. A common way of detecting faults in mechanical equipment, such as the suspension and chassis of a ground vehicle, is to compare measured vibrations to a reference (or healthy) signature to detect anomalies. In order to make this comparison, a library of vibration signatures must be developed and categorized according to the operational conditions of the vehicle

Report Documentation Page

Form Approved
OMB No. 0704-0188

1. REPORT DATE	2. REPORT TYPE	3. DATES COVERED
15 OCT 2008	**N/A**	**-**

4. TITLE AND SUBTITLE	5a. CONTRACT NUMBER
Health Monitoring for Condition-Based Maintenance of a HMMWV using an Instrumented Diagnostic Cleat	5b. GRANT NUMBER
	5c. PROGRAM ELEMENT NUMBER
6. AUTHOR(S)	5d. PROJECT NUMBER
Tiffany Dipetta; Nathanael Yoder; Douglas E. Adams; Joseph Gothamy; David Lamb; David Gorsich	5e. TASK NUMBER
	5f. WORK UNIT NUMBER
7. PERFORMING ORGANIZATION NAME(S) AND ADDRESS(ES)	8. PERFORMING ORGANIZATION REPORT NUMBER
US Army RDECOM-TARDEC 6501 E 11 Mile Rd Warren, MI 48397-5000	**19335RC**
9. SPONSORING/MONITORING AGENCY NAME(S) AND ADDRESS(ES)	10. SPONSOR/MONITOR'S ACRONYM(S)
	TACOM/TARDEC
	11. SPONSOR/MONITOR'S REPORT NUMBER(S)
	19335RC

12. DISTRIBUTION/AVAILABILITY STATEMENT

Approved for public release, distribution unlimited

13. SUPPLEMENTARY NOTES

Presented at 2009 SAE World Congress, April 2009, Detroit, Michigan, USA, The original document contains color images.

14. ABSTRACT

15. SUBJECT TERMS

16. SECURITY CLASSIFICATION OF:			17. LIMITATION OF ABSTRACT	18. NUMBER OF PAGES	19a. NAME OF RESPONSIBLE PERSON
a. REPORT	b. ABSTRACT	c. THIS PAGE			
unclassified	**unclassified**	**unclassified**	**SAR**	**9**	

Standard Form 298 (Rev. 8-98)
Prescribed by ANSI Std Z39-18

(speed, terrain, turning radius, etc.). Figure 1 illustrates this common approach to fault identification.

There are two principle difficulties with this approach. First, the number of datasets required to develop a library of possible healthy signatures extracted from an N-dimensional sensor suite on a vehicle given M terrains on which that vehicle can operate is of order M^N (Bishop, 1990). For example, 6 sensors over 10 terrains would require that one million datasets be used to establish a fully populated reference set for fault detection. If 240 datasets are acquired each day on average, then it would take 11 years to develop this library of healthy signatures for each individual ground vehicle. This large number of datasets would be needed to characterize the normal operational response of the vehicle due to the non-stationary nature of the loading and the inability to control these loads in operation. Second, many vehicles are not equipped with sensors nor the acquisition systems to acquire, process, and store data; therefore, to implement health monitoring for condition-based maintenance, one needs to overcome the economic and technical barriers associated with equipping ground vehicles to continuously monitor their responses.

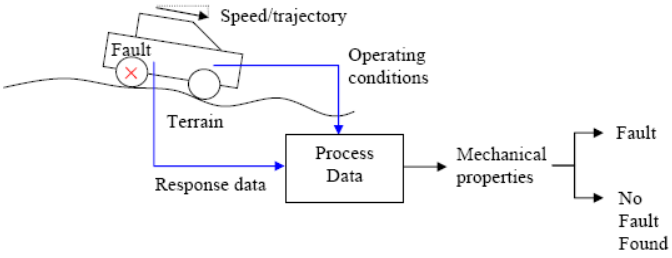

Figure 1: Illustration of common approach for diagnosing faults in ground vehicles using dynamic response and operational data.

To overcome these difficulties, it is useful to consider how rotating machinery diagnostic systems function. In these machines, the repetitiveness of the operating load for a machine operating at constant speed makes it relatively easy to identify faults in the bearings, shaft, etc. In wheeled ground vehicles, loading varies significantly as mentioned above. If loads acting on the vehicle could be fully measured or controlled in terms of the terrain input motions and/or spindle forces/moments, fault identification in wheeled vehicles at the component level would be more straightforward. Mechanical properties that determine the vehicle condition could be extracted from data if loads could be controlled.

There are two approaches being undertaken in this research that attempt to overcome the difficulties mentioned above:

(1) If a vehicle cannot be equipped with sensors, then an instrumented diagnostic cleat is proposed as illustrated in Figure 2 to measure the dynamic response of the vehicle as it traverses the cleat at a fixed speed. This approach could be effective because it eliminates the need for on-vehicle sensors.

(2) If a vehicle can be equipped with sensors, then a "reference-free" approach to data analysis is used to compare similar response pathways on the vehicle to identify mechanical anomalies. For example, the vertical and tracking responses of the left wheels can be compared to the same responses of the right wheels to determine if the front/rear wheels exhibit anomalies. This approach could be effective because it diminishes the need for reference signatures to identify faults; however, the approach is still somewhat sensitive to operational loading and variability.

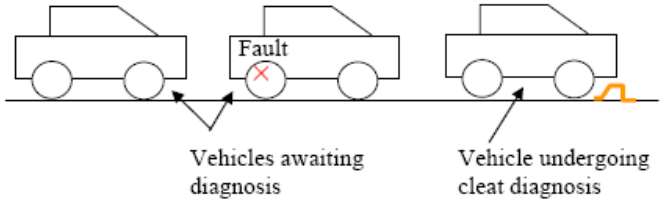

Figure 2: Illustration of concept for an instrumented cleat that diagnoses faults in wheel ends and suspensions of ground vehicle.

This paper investigates Approach (1). Some of the merits of this approach are as follows:

- Cleat is portable making it practical for field use.
- Cleat can be engineered to control the amplitude and frequency of the input imparted to the vehicle wheels allowing for more targeted diagnostic results.
- Vehicle speed traversing the cleat can be controlled.
- Configuration of cleats can be designed to develop specific tests for certain subsystems.
- Sensors are installed within the cleat rather than the vehicle providing greater reliability.
- Algorithms for analyzing response data from the cleat are less complex than for on-vehicle diagnostic algorithms, which must address non-stationary data.

First, a simplified half-car four degree of freedom model of a typical HMMWV (see Figure 2) is used to examine the sensitivity of measured forces in the tire to faults in the wheel and suspension. Second, a proof of concept experiment is conducted using an instrumented cleat to attempt to diagnose a fault in the strut coil spring.

LITERATURE REVIEW

The response of the HMMWV to a cleat excitation has been studied by Faller, Hillegass, and Docimo (2003). The response of the center of mass, driver, and left and right wheel of the HMMWV was experimentally determined with accelerometers during a road test over a 4 inch high semicircle cleat. The road test was conducted at vehicle speeds of 5 and 14 mph. The speed was found to affect the response of the vehicle.

Health monitoring systems usually place all measurement instrumentation on the vehicle itself to

measure vehicle responses. However, Champoux, Richard, and Drouet (2007) have used an instrumented cleat to study the wheel response of a bicycle. The cleat was instrumented with biaxial force transducers. The rest of the bicycle was instrumented with strain gages and accelerometers to measure the cyclist's comfort.

MODELING APPROACH

Dimensional and material data was obtained in the open literature regarding American General's standard HMMWV. Figure 1 shows a photo of the vehicle, which has been represented using a four degree of freedom lumped parameter model. It has a length of 4.6 m, width of 2.1 m, height of 1.8 m, and mass of 2340 kg. The frame is modeled as a rigid body with three lumped masses, M_j with j=1, 2, and 3, representing the front, rear, and center of mass payloads carried by the vehicle. The mass moment of inertia about the center of mass is I_{cm3}. Dimensions a and b describe the location of the center of mass. The tire stiffness properties are denoted by K_f and K_r for the front and rear wheels, respectively. K_1 and K_2 denote the front and rear suspension rate properties, respectively. Although not indicated in the schematic, proportional viscous damping is assumed in the model.

The vertical base motions of the front and rear tires are denoted by x_1 and x_2. The vertical and pitch motions of M_3 and I_{cm3} are denoted by x_3 and θ, respectively. The nominal parameter values that were used in the model are listed in Table 1.

Parameter	Value
M_1, M_2, M_3	950, 800, 1000 kg
M_f, M_r	100, 100 kg
I_{cm3}	10 kg·m^2
a, b	10, 5 ft
K_1, K_2	50000, 40000 N/m
K_f, K_r	500000, 400000 N/m

Table 1: Nominal parameter values in four degree of freedom model of HMMWV.

Figure 3: American General HMMWV for which model has been developed (Photo is a US Army work).

The lumped parameter set of differential equations corresponding to this model was derived using Newton-Euler methods and is given below:

$$\begin{bmatrix} M_1+M_2+M_3 & 0 & 0 & 0 \\ 0 & I_{cm3} & 0 & 0 \\ 0 & 0 & M_f & 0 \\ 0 & 0 & 0 & M_r \end{bmatrix} \begin{Bmatrix} \ddot{x}_3 \\ \ddot{\theta} \\ \ddot{x}_f \\ \ddot{x}_r \end{Bmatrix} + \begin{bmatrix} K_1+K_2 & * & * & * \\ -K_1(a+c)+K_2(b-c) & -K_1(a+c)+K_2(b-c) & * & * \\ -K_1 & K_1(a+c) & K_f+K_1 & * \\ -K_2 & -K_2(b-c) & 0 & K_r+K_2 \end{bmatrix} \begin{Bmatrix} x_3 \\ \theta \\ x_f \\ x_r \end{Bmatrix} = \begin{Bmatrix} 0 \\ 0 \\ K_f x_1 \\ K_r x_2 \end{Bmatrix} \tag{1}$$

where $c=(b \cdot M_2 - a \cdot M_1)/(M_1+M_2+M_3)$ and an "$*$" in the stiffness matrix indicates a symmetric entry in the matrix with respect to the diagonal. A viscous proportional damping model of the form,

$$[C] = \alpha[M] + \beta[K], \ \alpha = 0, \beta = 0.02 \tag{2}$$

is also used in Eq. (1) to describe the dissipative (non-conservative) effects. The functions x_1 and x_2 were used to model the profile of the cleat, which provides a base excitation to each wheel at different times. x_1 and x_2 were expressed using a Hanning function of the form:

$$x_1(t) = \begin{cases} \frac{h}{2}\left(1-\cos\frac{2\pi t}{T_c}\right) & \text{for } t \le T_c \\ 0 & \text{for } t > T_c \end{cases}$$
$$x_2(t) = x_1(t - T_b) \tag{3}$$

where h is the height of the cleat, T_c is the time during which a wheel is in contact with the cleat, and T_b is the time it takes for the rear wheel to come into contact with the cleat after the front wheel has reached the cleat. This approach was used because experimentally the measurement would be triggered at t=0 sec once the front wheel reaches the cleat. T_c can be calculated using the length of the cleat L and the speed of the vehicle v, $T_c = L/v$. Likewise, T_b can be calculated using the distance from wheel to wheel (wheelbase) w and the speed, $T_b = w/v$. x_1 and x_2 are plotted in Figure 5 for a 15 ft wheelbase, 12 in wide cleat, and speed of 5.8 mph. Part of the instrumented cleat design is associated with the frequency range over which these cleats excite the vehicle. Therefore, the frequency spectra of these base excitation time histories are also plotted in Figure 6. Both inputs produce the same spectral features because

they are identical in amplitude but different in phase. The bandwidth of these excitations is 94 rad/s.

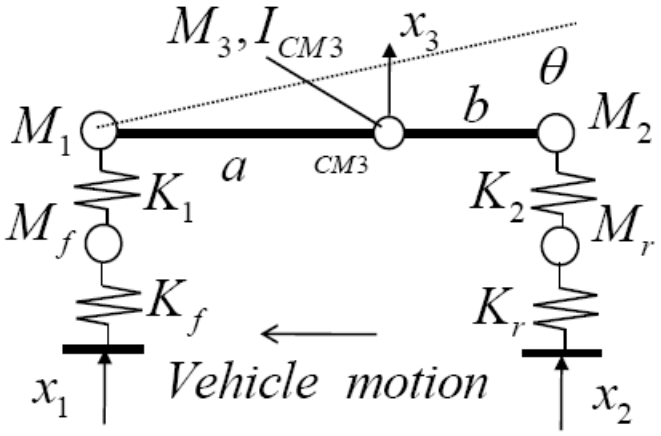

Figure 4: Simplified four degree of freedom model for HMMWV showing wheels and suspension on front and rear of vehicle.

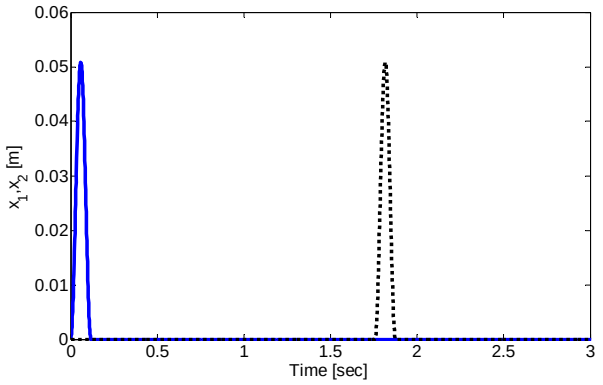

Figure 5: x_1 and x_2 cleat inputs acting on front (▬) and rear (▪ ▪ ▪) tires.

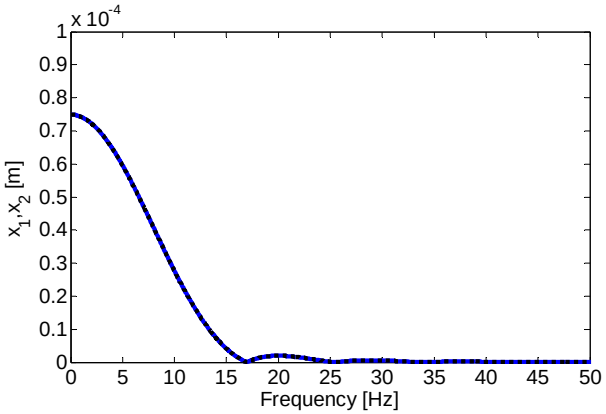

Figure 6: $X_1(f)$ and $X_2(f)$ cleat inputs acting on front (▬) and rear (▪ ▪ ▪) tires.

The input-output model in Eq. (1) was then rewritten in state variable form in preparation for conducting time-domain simulations. The state vector in this state space representation of the model consisted of the response vector from Eq. (1) and its derivative. The state variable model is given by,

$$\frac{d}{dt}\begin{Bmatrix}\{x\}\\ \{\dot{x}\}\end{Bmatrix} = \begin{bmatrix}[0]_{4\times4} & [I]_{4\times4}\\ -[M]^{-1}[K] & -[M]^{-1}[C]\end{bmatrix}\begin{Bmatrix}\{x\}\\ \{\dot{x}\}\end{Bmatrix}$$

$$+\begin{bmatrix}[0]_{6\times2} & [0]_{6\times2}\\ \begin{bmatrix}M_f & 0\\ 0 & M_r\end{bmatrix}^{-1}\begin{bmatrix}K_f & 0\\ 0 & K_r\end{bmatrix} & \begin{bmatrix}M_f & 0\\ 0 & M_r\end{bmatrix}^{-1}\begin{bmatrix}\beta K_f & 0\\ 0 & \beta K_r\end{bmatrix}\end{bmatrix}\begin{Bmatrix}x_1(t)\\ x_2(t)\\ \dot{x}_1(t)\\ \dot{x}_2(t)\end{Bmatrix} \quad (4)$$

The desired outputs of this model are the forces inside the front and rear tires because the goal of the instrumented cleat is to measure forces in the tire to identify faults in the tires and suspension. Therefore, the output equation used in this state variable model is given by:

$$\begin{Bmatrix}f_1\\ f_2\end{Bmatrix} = \begin{bmatrix}0 & 0 & -K_f & 0 & 0 & 0 & -\beta K_f & 0\\ 0 & 0 & 0 & -K_r & 0 & 0 & 0 & -\beta K_r\end{bmatrix}\begin{Bmatrix}\{x\}\\ \{\dot{x}\}\end{Bmatrix} + \begin{bmatrix}K_f & 0 & \beta K_f & 0\\ 0 & K_r & 0 & \beta K_r\end{bmatrix}\begin{Bmatrix}x_1(t)\\ x_2(t)\\ \dot{x}_1(t)\\ \dot{x}_2(t)\end{Bmatrix} \quad (5)$$

ANALYSIS

UNDAMAGED SYSTEM (MODAL PROPERTIES)

The modal properties associated with the free response of the vehicle model were calculated by solving the corresponding eigenvalue problem using the state matrix in Eq. (4). The eigenvalue formulation takes the following form:

$$\begin{bmatrix}[0]_{4\times4} & [I]_{4\times4}\\ -[M]^{-1}[K] & -[M]^{-1}[C]\end{bmatrix}\begin{Bmatrix}\{x\}\\ \{\dot{x}\}\end{Bmatrix} = \lambda\begin{Bmatrix}\{x\}\\ \{\dot{x}\}\end{Bmatrix} \quad (6)$$

where $\{x\}$ is the modal deflection shape and λ is the corresponding modal frequency (eigenvalue). For the mechanical properties chosen in Table 1, the eigenvalue problem in Eq. (6) was solved and the modal properties obtained are listed in Table 2. The first two modes of vibration are associated with the sprung mass (pitch and bounce) and the second two modes are associated with the wheel hop resonances of the front and rear. The modal deflection shapes are only indicated to two significant digits to highlight the dominant degrees of freedom in each mode shape. The four undamped

natural frequencies are at 0.63, 0.88, 7.90, and 7.92 Hz. Consequently, when the base excitation functions shown in Figure 6 are applied to the vehicle moving at 5.8 mph, all four modes of vibration will be excited because the bandwidth of the primary lobes in each of the input frequency spectra spans the frequency range from 0 to 15 Hz (94 rad/s). If the vehicle is traveling more slowly, it is possible that all modes of vibration will not be excited in the forces that are measured in the tires.

Undamped Freq. (rad/s) and Damping Ratio	**Modal Vector (Two significant digits)**
4.0, 0.04	$[0.87\ 1.00\ -0.14\ -0.27]^T$
5.5, 0.06	$[1.00\ -0.09\ 0.11\ 0.07]^T$
49.6, 0.89	$[-0.00\ -0.00\ -0.00\ 1.00]^T$
49.7, 1.11	$[-0.00\ 0.00\ 1.00\ 0.00]^T$

Table 2: Modal parameters of HMMWV four degree of freedom model.

UNDAMAGED SYSTEM (BODE DIAGRAMS)

To examine the forces that are produced in the tires of the vehicle as the front and rear wheels traverse the cleat, the Bode diagrams relating the input displacements to the wheels (x_1 and x_2) and the forces in the tires (f_1 and f_2, see Eq. (5)) were constructed. These bode diagrams relate the amplitudes and phases of the input displacements to the amplitudes and phases of the forces measured within the instrumented cleat, which is proposed for use in diagnosing vehicle faults. Figure 7 shows the Bode diagrams for the four frequency response functions relating the tire input displacements to the tire output forces.

The modal frequencies given above for the sprung vehicle mass are evident in the peaks of the Bode magnitude plots. The two wheel hop frequencies are also evident but are much more heavily damped than the bounce and pitch modes as expected from Table 2.

DAMAGED SYSTEM (BODE DIAGRAMS)

Damage due to fractured suspension tie bolts or faulty struts and tires that are underinflated or contain separated plies are analyzed in this work. First, a 15% reduction in K_1 (see Figure 4) is used to model damage in the front suspension. Figure 8 shows the resulting Bode diagram relating the input displacement at the front wheel to the force in the front tire in the undamaged (—) and damaged (– – –) states. The frequency range most sensitive to this damage is the mid-frequency range in the vicinity of the resonances of the sprung mass.

This result is consistent with the location of the damage in the system relative to the deflection mode shapes listed in Table 2. It is evident from the bounce motion at 4 rad/s (and to a lesser extent in the pitch motion at 5 rad/s) that there is more deflection and velocity across the suspension than in the tire hop deflections. Therefore, these motions of the sprung mass are most sensitive to the suspension damage in K_1. In contrast, the response in the frequency range above 40 rad/s is most sensitive to changes in the front tire rate, K_f.

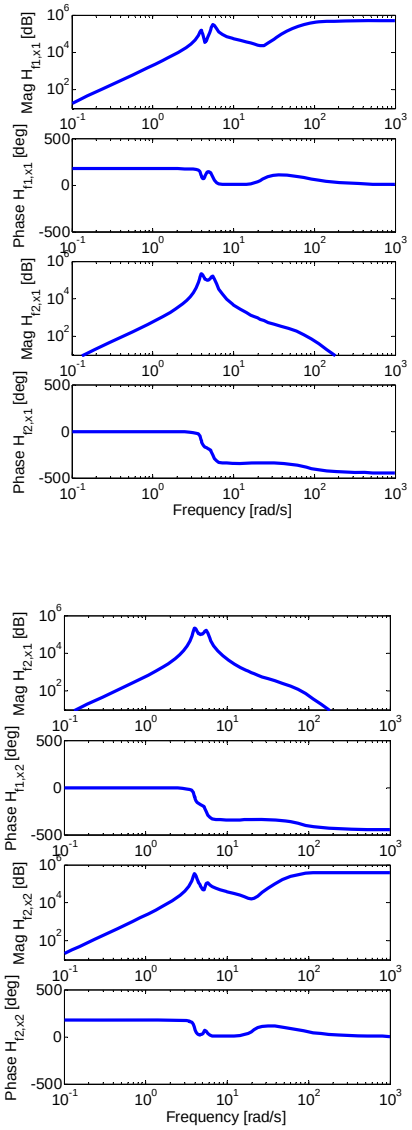

Figure 7: Bode diagrams (magnitude and phase) for the following output/input frequency response functions: (a) F_1/X_1, (b) F_2/X_1, (c) F_1/X_2, and (d) F_2/X_2.

DAMAGED SYSTEM (FORCED RESPONSE)

The damage mechanisms in the front suspension and tire that were simulated in the previous section were again introduced in this section. The forced response in the time and frequency domains for the excitation functions shown in Figure 5 was then calculated. Figure 9 shows the time and frequency domain forces in the front tires for the fault scenario involving a 15% reduction in the front suspension system. In Figure 9(a,b), two sets of forces in the time and frequency domains in the tire are plotted. The solid lines correspond to tire forces in the undamaged (—) and

damaged ( ) vehicle assuming the force can only be measured while the tire is traversing the cleat. The dotted lines correspond to the same scenario assuming the force can be measured throughout the entire time period shown. It is evident that there are subtle changes in the time history due to a fault and more pronounced changes in the frequency spectrum. It is interesting to note that the primary changes in the spectrum occur in the frequency range dominated by the pitch and bounce degrees of freedom due to the previous conclusion about the sensitivity of the force in the tire to faults in the vehicle (see Figure 8).

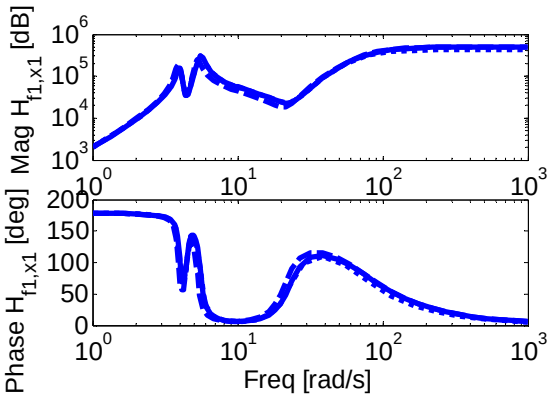

Figure 8: Magnitude and phase of Bode diagram for input at front wheel and output force in front tire for undamaged case ( ), damage in front suspension ( ), and damage in front wheel ( ) showing frequency ranges sensitive to damage.

The same forced response simulation was performed for a scenario involving a 15% reduction in the front tire stiffness. Then the resulting forced response for this fault in addition to the forced response for the suspension fault were both subtracted from the undamaged forced response. The spectral magnitudes of these differences due to the two distinct faults were plotted as shown in Figure 10 out to 200 rad/s. The effects of the suspension fault ( ) and tire fault ( ) affect different frequency ranges as explained in Figure 8. Moreover, the suspension fault exhibits larger changes in the low frequency range whereas the tire fault exhibits larger changes in the high frequency range. When the entire force time history is measured throughout the vehicle motion, the differences due to faults are more apparent. However, the differences are also apparent in the case when only the short segment of force data is available as the tires traverse the cleat.

To examine the effects of a change in the aspect ratio of the cleat, the width was increased by a factor of 2 (24 in) and 3 (36 in), and the change in force was again calculated for the scenario involving only a fault in the front tire. The percentage change in force spectrum was then plotted in Figure 11 for the case when the force is measured in the tire throughout the entire vehicle travel. The figure shows that as the width of the cleat becomes larger for a fixed height, the sensitivity to the tire fault increases throughout the entire frequency range. A wider cleat places more of the excitation in the lower frequency range resulting in larger amplitudes of displacement across the wheels and struts, which increases the sensitivity to faults in the tire. For the suspension fault, the increase in sensitivity is also noticeable for wider cleats but only in the low frequency range below 5 rad/s. These results suggest that for a given height, changes in the width of the cleat affect the sensitivity of the measured force in the cleat to tire faults more than to suspension faults.

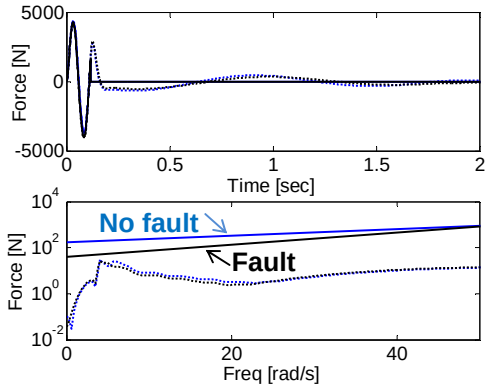

Figure 9: Forced response in the (a) time and (b) frequency domains with ( ) and without ( ) a fault introduced in the front suspension using the complete ( ) and partial ( ) force time histories.

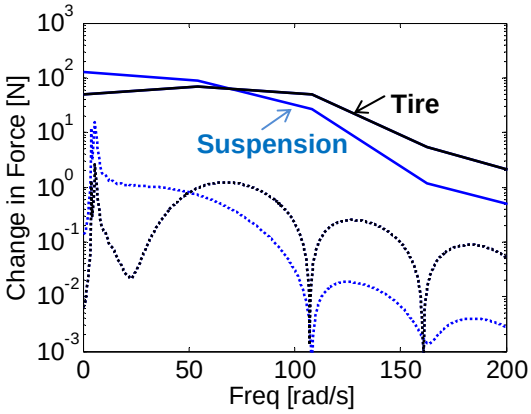

Figure 10: Magnitude of change in force for a suspension ( ) and tire ( ) fault using the complete ( ) and partial ( ) force time histories.

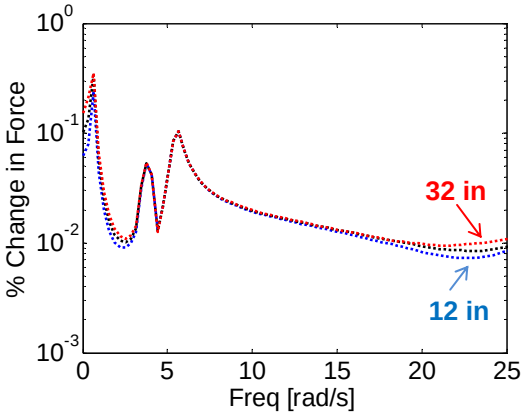

Figure 11: Percentage change in magnitude of change in force for a front tire fault for a 12 in (▪ ▪ ▪), 24 in (▪ ▪ ▪), and 32 in (▪ ▪ ▪) wide cleat using the complete force time histories.

EXPERIMENTAL VALIDATION

To validate the analytical findings, a rubberized cleat was instrumented with two PCB 356B18 tri-axial accelerometers and a small truck was used as the test vehicle. These accelerometers were used to measure the responses on the left and right side of the cleat. These responses are indicative of the forcing function that acts through the tire as the vehicle traverses the cleat. The accelerometers were positioned in the center plane of the cleat using metal plugs and cables were run out to the data acquisition system through the base of the cleat. The plugs were installed so that they were not touching the ground to provide measurements that would be sensitive to the forces acting through the tire. The instrumented cleat used in the experiment is shown in Figure 12(a) with a close up of one of the accelerometers and plugs in Figure 12(b).

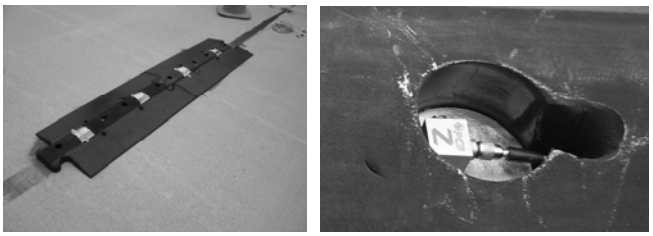

Figure 12: (a) Instrumented cleat used in experiments, and (b) tri-axial accelerometer installed inside cleat.

The experiment consisted of six tests: a first baseline, a simulated suspension fault, three simulated tire faults, and a second baseline. The baseline vehicle had no faults and the pressure in all four tires was 35psi. The fault in the vehicle suspension was simulated by inserting a metal spacer into the front right coil spring of the vehicle as shown in Figure 13. The three different tire faults were simulated by reducing the pressure of the front right tire to 30psi, 25psi, and 20psi.

Figure 13: Metal spacer inserted into coil to simulate suspension fault.

Each test consisted of the vehicle being driven over the instrumented cleat at 5 mph five times and the average accelerations were calculated from the measure data. The data was initially sampled at 16,384 Hz and then down sampled to 819.2 Hz to highlight the lower frequency content that is more indicative of the wheel end and suspension response. Figure 14 shows the (a) right and (b) left cleat responses in the vertical, lateral, and tracking directions for the first baseline measurement as the front tire traversed the cleat. The time histories observed when the back wheels traversed the cleat were similar. Note that the left cleat measurement was slightly delayed by 70 msec relative to the right cleat measurement. The reason for this delay is that the two tires strike the cleat at slightly different times. The response amplitudes in the three directions were different with a peak acceleration of 1.5 g.

First, the suspension fault simulated as shown in Figure 13 was considered. Figure 15 shows the vertical acceleration spectra for the (a) right and (b) left wheels.

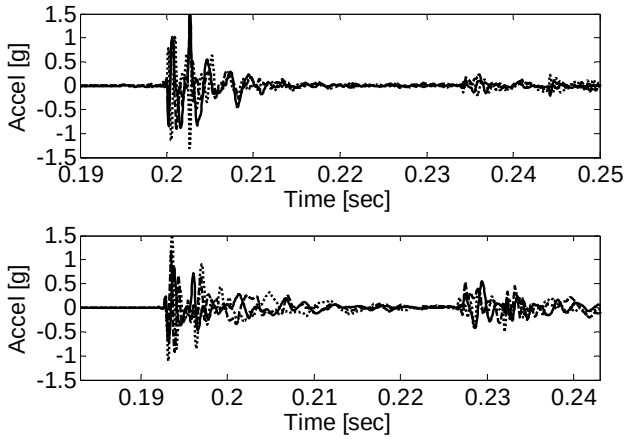

Figure 14: Acceleration responses on (a) right and (b) left sides of instrumented cleat with (▬) vertical, lateral (▬ ▬), and tracking (▪ ▪ ▪) directional responses with 35 psi tire pressure and 5 mph.

These plots correspond to the data acquired as the front wheels traversed the cleat. The solid dark (▬) and dotted dark (▪ ▪ ▪) lines correspond to the two baseline datasets. The lighter solid line (▬) corresponds to the suspension fault dataset. Note that on the top plot for the right wheel in Figure 15(a), the suspension fault data exhibits two strong peaks at 7.5 and 15 Hz, respectively. The peak at 7.5 Hz is associated with one of the suspension modes probably at 10 Hz in the other two datasets. The modal peak when the metal spacer is inserted is lower in frequency because by splitting the coil spring of stiffness k into two shorter coil springs of stiffness k, the resultant effective stiffness of the spring is lower, e.g., k/2. The peak at 15 Hz is a second harmonic of 7.5 Hz due to the nonlinear response of the suspension as the spring coils compress on the metal spacer. This behavior was not modeled in the simplified model of Figure 4; however, nonlinear behavior is expected in the suspension for this type of fault. In contrast, the data in Figure 15(b) for the left wheel does not exhibit significant differences between the two

baseline datasets and the faulty dataset. To quantify these differences, the difference between the second baseline dataset and the first baseline dataset and the difference between the faulty dataset and the first baseline dataset were calculated as a function of frequency. Then the area underneath these two functions were calculated and plotted as a function of frequency. Figure 16 shows this fault index. Note that the faulty dataset exhibits a larger difference from the first baseline dataset than the second baseline dataset. An appropriate threshold would need to be chosen in order to detect the suspension fault using this result.

To verify that this approach is effective at isolating the fault, the data was also analyzed as the rear wheel traversed the cleat. Figure 17 shows the comparison of the spectra. Note that now there is no indication that the faulty dataset is significantly different from the baseline datasets. This result verifies that the fault is indeed in the front suspension as opposed to the rear suspension.

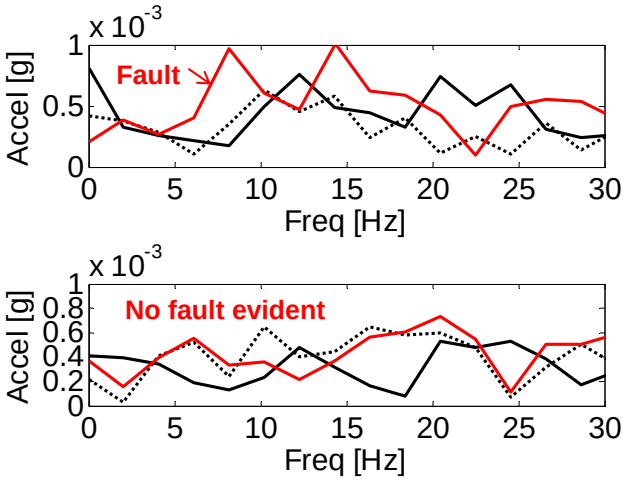

Figure 15: Front vertical acceleration responses on (a) right and (b) left sides of instrumented cleat with (▬) first baseline, (▪▪▪) second baseline, and (▬) faulty datasets indicating fault near 7.5 and 15 Hz.

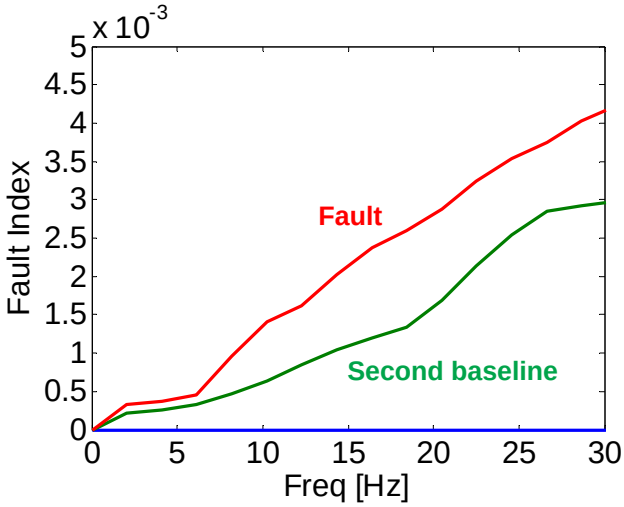

Figure 16: Comparison of fault index for second baseline dataset (▬) and faulty dataset (▬) indicating larger differences due to the fault than due to measurement variability.

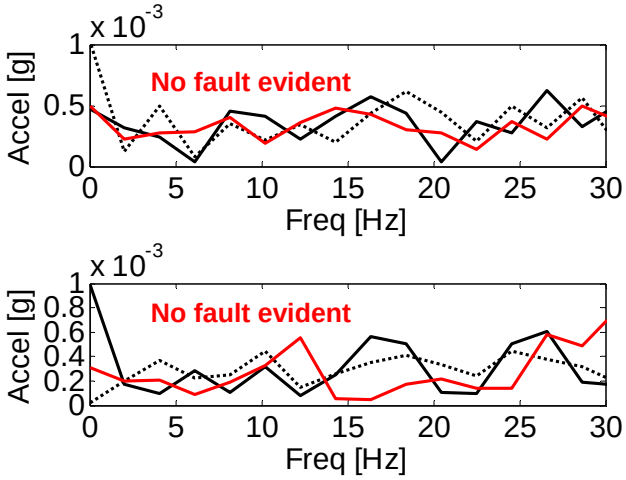

Figure 17: Rear vertical acceleration responses on (a) right and (b) left sides of instrumented cleat with (▬) first baseline, (▪▪▪) second baseline, and (▬) faulty datasets indicating no fault.

CONCLUSION

A simplified four degree of freedom model of a HMMWV was developed to study changes in the forces in the tires as a function of faults in the wheels and suspensions. Simulations showed that tire faults were more readily detected than suspension faults at lower frequencies using measured forces in a roadway cleat. Longer cleats were shown to produce data that better separated healthy and faulty wheel end and suspension responses. Tests on a small truck showed that a simulated suspension fault could be detected and isolated to the front right corner of the suspension using an instrumented rubberized cleat to measure tire forces.

REFERENCES

1. Gorsich, D., “Reliability Centered Maintenance,” 2007, Condition-Based Maintenance Workshop, Tank Automotive Research Development Engineering Center, Warren, MI.
2. Thomas, M., “Major Ground Equipment System Accidents Caused by Materiel Failure,” 1985, TN 85-3.
3. Aardema, J., “Failure Analysis of the Lower Rear Ball Joint on the HMMWV,” 1988, AD-1201 894.
4. Lasure, Maj. K., “Pilot RCM I HMMWV Analysis,” 2004.
5. FORSCOM Safety Alert Message, TACOM SOUM 04-017, 2004.
6. Bishop, C. M., “Neural Networks for Pattern Recognition,” 1995, Clarendon Press, Oxford.

DEFINITIONS, ACRONYMS, ABBREVIATIONS

CBM: Condition Based Maintenance

HMMWV: High Mobility Multipurpose Wheeled Vehicle